Journal of Ceramic Processing Research. Vol. 18, No. 5, pp. 394~398 (2017)

JOURNAL OF
Ceramic Processing Research

Structural and magnetic properties of Ni substituted M-type Ca-Sr hexaferrites synthesized by solid-state reactions

Yujie Yang*, Juxiang Shao, Fanhou Wang and Duohui Huang

Computational Physics Key Laboratory of Sichuan Province, School of Physics and Electronic Engineering, Yibin University, Yibin 644007, P. R. China

In this study, we have prepared the M-type Ca-Sr hexaferrites with composition of $Ca_{0.2}Sr_{0.8}Fe_{12.0-x}Ni_xO_{19}$ ($0.0 \le x \le 0.8$) by the solid-state reactions. The phase compositions of the samples were confirmed by X-ray diffraction analysis. The results of X-ray diffraction patterns show that for the M-type hexaferrite magnetic powders with the Ni content (x) from 0.0 to 0.4, the XRD patterns belong to the M-type strontium hexaferrite; when Ni content (x) ≥ 0.6, $Sr_4Fe_6O_{13}$ is detected. It is observed that lattice parameter *c* first increases with the increase of Ni content (x) from 0 to 0.4, and then decreases when Ni content (x) ≥ 0.4, while lattice parameter *a* basically keeps constant. Magnetization properties were measured at room temperature by a permanent magnetic measuring system. The remanence (B_r) first increases with increasing Ni content (x) from 0.0 to 0.2, and then decreases when Ni content (x) ≥ 0.2. The the intrinsic coercivity (H_{cj}), magnetic induction coercivity (H_{cb}) and maximum energy product [$(BH)_{max}$] decrease with the increase of Ni content (x) from 0.0 to 0.8.

Key words: M-type hexaferrites, Ni substitution, X-ray diffraction, Magnetic properties.

Introduction

M-type hexaferrites are the earliest developed material of the class of hexagonal ferrite. The materials are perfect chemical stability, and have strong uniaxial anisotropy, moderate energy product, and high Curie temperature [1]. The magnetic properties of M-type hexaferrites can be modified by the ion substitution. The substitutions of rare earth metals, such as La^{3+}, Pr^{3+}, Nd^{3+}, or transition metals, such as Co^{2+}, Mn^{3+}, and Al^{3+} have been investigated by several researchers [2-7]. Seifert et al. have synthesized the single-phase hexagonal ferrites $Sr_{1-x}La_xFe_{12}O_{19}$ ($0 \le x \le 1$) by a ceramic route and found that the saturation magnetization at $T = 5$ K decreases with the increase of La concentration [2]. Sharma et al. have studied the Mn ions substituted M-type barium hexaferrite powders $BaFe_{12-x}Mn_xO_{19}$ ($0 \le x \le 0.50$), and found that with increasing Mn ion content, the crystallite size was found to decrease and the saturation magnetization reduced while coercivity increased [6]. Combined substitutions, such as La-Co, La-Cu, Ce-Co, Co-W, Bi-Cr, Mn-Zn, and Al-Cr have been reported [8-14]. Yang et al. have studied the La-Cu doped M-type hexaferrites $Sr_{1-x}La_xFe_{12-x}Cu_xO_{19}$ ($0.0 \le x \le 0.35$) prepared by the ceramic process and found that with the remanence and maximum energy product first increase with x from 0 to 0.20, and then decrease when $x \ge 0.2$, while the intrinsic coercivity and magnetic induction coercivity decrease linearly with increasing x from 0 to 0.35 [9]. Shakoor et al. have synthesized the Bi-Cr substituted strontium hexaferrite nanoparticles $SrFe_{12-2x}(BiCr)_xO_{19}$ (x = 0.2, 0.4, 0.6, 0.8) by the sol-gel method and found that the saturation magnetization and remanence increase with increasing the dopant concentration up to $x = 0.2$ and then decrease with further increase in dopant content, while coercivity decreases with increasing the dopant content up to x = 0.2 and then increases with further increase in dopant content [12].

The magnetic properties of M-type hexaferrites can be affected by the preparation methods, and experimental conditions. Studies on the Ni substituted M-type hexaferrites are very few. Thus, in the present investigation, Ni^{2+} ions are chosen to substitute the Fe^{3+} ions. We have prepared the Ni substituted M-type Ca-Sr hexaferrites by the solid-state reactions. The aim of the present study is to investigate the influence of Ni content on the microstructure and magnetic properties.

Experimental Procedure

The M-type Ca-Sr hexaferrites with composition of $Ca_{0.2}Sr_{0.8}Fe_{12.0-x}Ni_xO_{19}$ (x = 0.0, 0.2, 0.4, 0.6, 0.8) have been prepared by the solid-state reactions. The raw materials, $CaCO_3$, $SrCO_3$, Fe_2O_3 and NiO, all 99% pure, were weighted with the design ratios. The raw materials were wet-mixed in a ball mill. After that, the mixed powders were dried in a drying oven, and pre-sintered at 1250 °C in air for 2.0 hrs. Then the pre-

*Corresponding author:
Tel : +86-831-3531171
Fax: +86-831-3531161
E-mail: loyalty-yyj@163.com

sintered powders were shattered to particles less than 60 μm, and then wet-milled with suitable additives ($CaCO_3$, $SrCO_3$, SiO_2, and Al_2O_3) for 16 h. Finally, the finely milled slurry was pressed into cylindrical pellets (diameter 30 mm, thickness about 16 mm) in the magnetic field of 800 kA/m. The pressed pellets were sintered at 1190 °C in air for 1.5 hrs. In order to measure the magnetic properties, the sintered pellets were polished in the faces perpendicular to the pressing direction.

For the phase identification of the samples, X-ray diffraction (XRD) measurements were performed on the X-ray diffractometer (SmartLab 9 kW, made by the Rigaku Corporation) with Cu $K_\alpha(\lambda = 1.5406$ Å) radiation. The lattice constants (c and a) are calculated from the XRD data by using the following equation [15]:

$$\frac{1}{d_{hkl}^2} = \frac{4}{3} \times \frac{h^2+hk+k^2}{a^2} + \frac{l}{c^2} \quad (1)$$

where d_{hkl} is the inter-planer spacing value, and h, k and l are corresponding Miller indices. The magnetic properties of the sintered pellets were measured at room temperature by a permanent magnetic measuring system (NIM-2000HF, made by the National Institute of Metrology of China).

Results and Discussion

Fig. 1 shows the X-ray diffraction patterns of the Ni substituted M-type hexaferrite $Ca_{0.2}Sr_{0.8}Fe_{12.0-x}Ni_xO_{19}$ magnetic powders with Ni content (x) from 0.0 to 0.8. It is seen that for the M-type hexaferrite magnetic powders with the Ni content (x) from 0.0 to 0.4, the XRD patterns belong to the M-type strontium hexaferrite (JCPDS card no. 80-1198). For the magnetic powders with the Ni content (x) from 0.6 to 0.8, $Sr_4Fe_6O_{13}$ is detected in the structure.

The lattice parameters (c and a) are calculated from the XRD data according to equation (1). The change of lattice parameters (c and a) of the M-type hexaferrite $Ca_{0.2}Sr_{0.8}Fe_{12.0-x}Ni_xO_{19}$ with Ni content (x) from 0.0 to 0.8 is shown in Fig. 2. In the present study, Ni^{2+} ion substitutes Fe^{3+} ion. It is seen that lattice parameter c first increases with the increase of Ni content (x) from 0 to 0.4, and then decreases when Ni content (x) ≥ 0.4, while lattice parameter a basically keeps constant. The increase of lattice parameter c with Ni content (x) from 0.0 to 0.4 is mainly due to the fact that the ionic radius of Ni^{2+} ion (0.69 Å) is bigger as compared to the ionic radius of Fe^{3+} ions (0.645 Å). When Ni content (x) ≥ 0.4, the impurity phase $Sr_4Fe_6O_{13}$ may cause lattice distortion. This should be the reason for the decrease of lattice parameter c.

The variation of c/a ratios as a function of Ni content (x) for the M-type hexaferrite $Ca_{0.2}Sr_{0.8}Fe_{12.0-x}Ni_xO_{19}$ is shown in Fig. 3. It is noted that c/a ratios of M-type

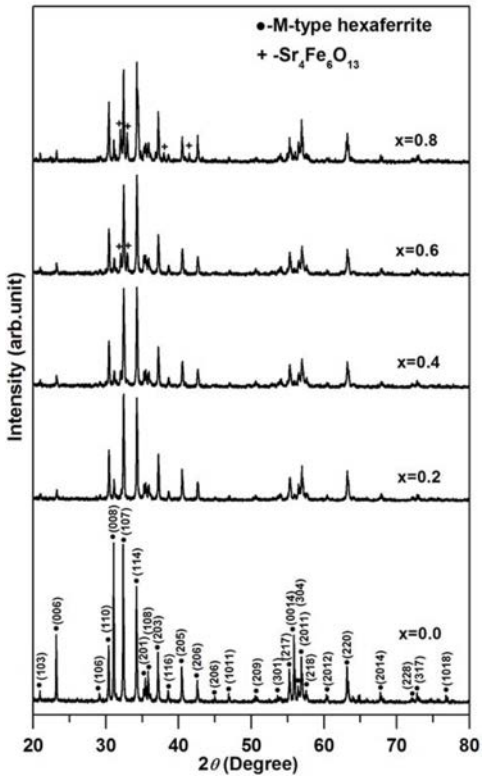

Fig. 1. XRD patterns of the Ni substituted M-type hexaferrite $Ca_{0.2}Sr_{0.8}Fe_{12.0-x}Ni_xO_{19}$.

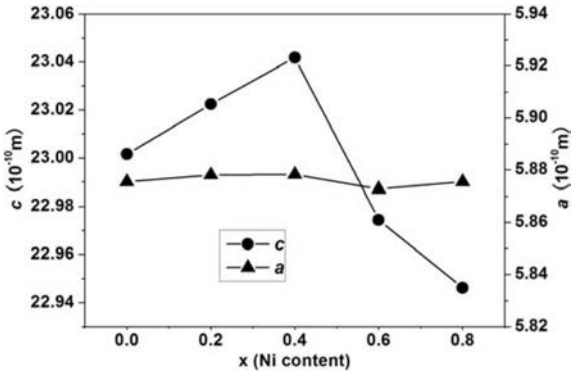

Fig. 2. Lattice parameters (c and a) of the M-type hexaferrite $Ca_{0.2}Sr_{0.8}Fe_{12.0-x}Ni_xO_{19}$ with Ni content (x) from 0.0 to 0.8.

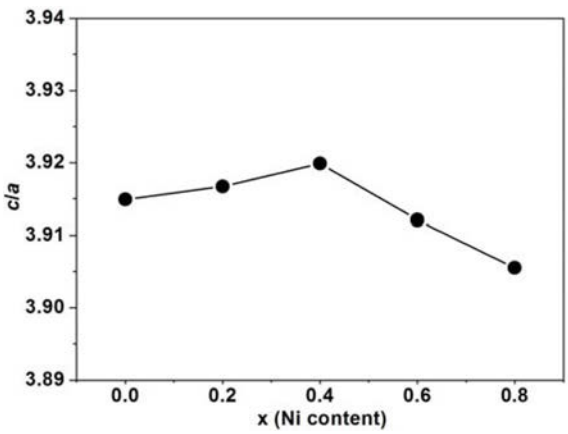

Fig. 3. c/a ratios as a function of Ni content (x) for the M-type hexaferrite $Ca_{0.2}Sr_{0.8}Fe_{12.0-x}Ni_xO_{19}$.

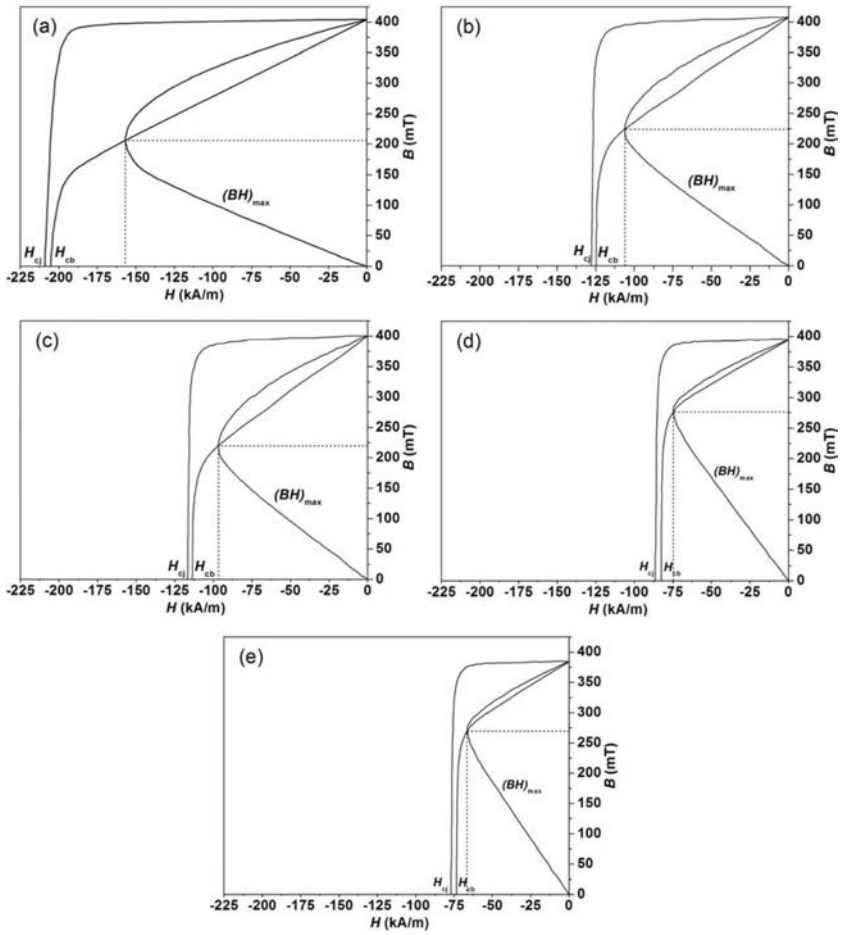

Fig. 4. Demagnetizing curves of the M-type hexaferrite $Ca_{0.2}Sr_{0.8}Fe_{12.0-x}Ni_xO_{19}$ magnets with different Ni content (x) measured at room temperature.

hexaferrites first slightly increases with increasing Ni content (x) from 0.0 to 0.4, and then decreases when Ni content (x) ≥ 0.4. The lattice parameter ratio *c*/*a* can be used to quantify the structure type, and an M-type structure can be assumed if the ratio is lower than 3.98 [16]. The *c*/*a* ratios with different Ni contents are in the range from 3.9149 to 3.9199, which confirms the formation of M-type hexagonal structure.

Fig. 4 shows the demagnetizing curves of the M-type hexaferrite $Ca_{0.2}Sr_{0.8}Fe_{12.0-x}Ni_xO_{19}$ magnets with different Ni content (x) measured at room temperature. The remanence (B_r), the intrinsic coercivity (H_{cj}), magnetic induction coercivity (H_{cb}) and maximum energy product [$(BH)_{max}$] are extracted from the demagnetizing curves.

The variation of remanence (B_r) as a function of Ni content (x) for the M-type hexaferrite $Ca_{0.2}Sr_{0.8}Fe_{12.0-x}Ni_xO_{19}$ magnets are shown in Fig. 5. It is seen from Fig. 5 that B_r first increases with increasing Ni content (x) from 0.0 to 0.2, and then decreases when Ni content (x) ≥ 0.2. In the M-type hexaferrites, Fe^{3+} ions occupy five different crystallographic sites: three octahedral sites (12k, $4f_2$ and 2a), one geometric tetrahedron site ($4f_1$), and one bipyramidal site (2b). 2a, 2b and 12k are spin up sites, whereas $4f_1$ and $4f_2$ are spin down sites [7]. Rane et al have reported that Ni^{2+} ions occupy octahedral site $4f_2$ at lower substitution and occupy octahedral site 12k at higher substitution [17]. Therefore, the increase of remanence (B_r) with with increasing Ni content (x) from 0.0 to 0.2 can be due to the following reason. When Ni content (x) ≤ 0.2, Ni^{2+} ions occupy spin down site $4f_2$, and as a result the total number of spin in the

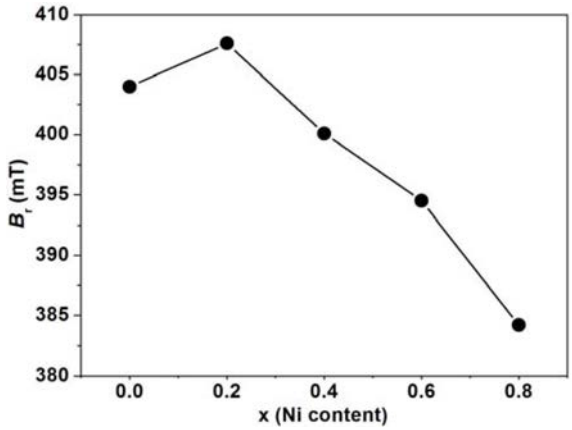

Fig. 5. Rmanence (Br) as a function of Ni content (x) for the M-type hexaferrite Ca0.2Sr0.8Fe12.0-xNixO19 magnets.

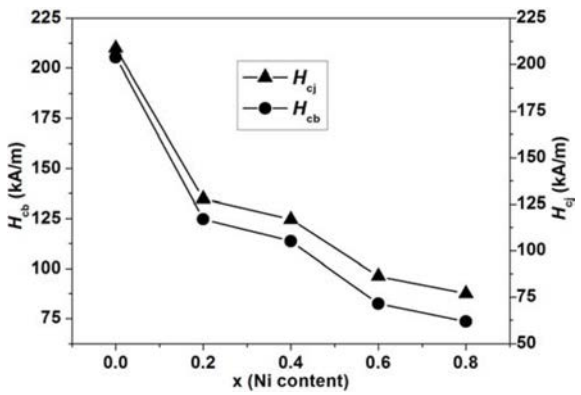

Fig. 6. Intrinsic coercivity (H_{cj}) and magnetic induction coercivity (H_{cb}) as a function of Ni content (x) for the M-type hexaferrite $Ca_{0.2}Sr_{0.8}Fe_{12.0-x}Ni_xO_{19}$ magnets.

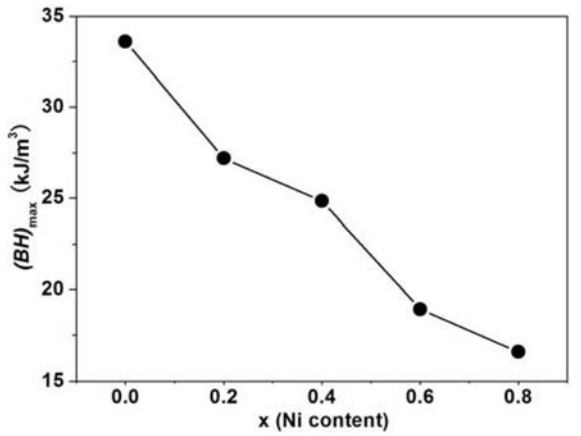

Fig. 7. Maximum energy product [$(BH)_{max}$] as a function of Ni content (x) for the M-type hexaferrite $Ca_{0.2}Sr_{0.8}Fe_{12.0-x}Ni_xO_{19}$ magnets.

spin up direction will increase because of the Ni^{2+} ion has lower magnetic moment (2 μ_B) than that of Fe^{3+} (5 μ_B). Consequently, the remanence (B_r) increases. The decrease of remanence (B_r) when Ni content (x) $\geq$ 0.2 can be due to the below two reasons. Firstly, with the doping of Fe^{3+} (5 μ_B) ions in the 12k sites by Ni^{2+} (2 μ_B), the Fe^{3+}-O-Fe^{3+} superexchange interaction is weakened, which causes to magnetic collinearity to collapse. This results in the degradation of remanence (B_r). Secondly, for the Ni substituted M-type hexaferrites when Ni content (x) $\geq$ 0.6, the decrease of remanence (B_r) could be attributed to the appearance of impurity phase as shown in Fig. 1. In M-type hexaferrites, the impurity phase has almost no contribution to the increase of remanence (B_r).

Fig. 6 shows the variations of intrinsic coercivity (H_{cj}) and magnetic induction coercivity (H_{cb}) as a function of Ni content (x) for the M-type hexaferrite $Ca_{0.2}Sr_{0.8}Fe_{12.0-x}Ni_xO_{19}$ magnets. It is found from Fig. 6 that both H_{cj} and H_{cb} decrease with the increase of Ni content (x) from 0.0 to 0.8. According to the Stoner-Wohlfarth theory, the coercivity in the M-type hexaferrite could be estimated by the below equation [18]:

$$H_c = 0.64\frac{2K}{M_s} \tag{2}$$

where K is the magnetocrystalline anisotropy constant and M_s is the saturation magnetization. Therefore, according to the equation (2), the decrease of H_{cj} should be due to be due to the decrease of uniaxial anisotropy constant because of the occupancy of the $4f_2$ and 12k sites by Ni^{2+} ions.

Fig. 7 shows the change of the maximum energy product [$(BH)_{max}$] with Ni content (x) for the M-type hexaferrite $Ca_{0.2}Sr_{0.8}Fe_{12.0-x}Ni_xO_{19}$ magnets. It is seen that the value of $(BH)_{max}$ decrease with the increase of Ni content (x) from 0.0 to 0.8. The maximum energy product of the hexaferrite magnets can be estimated by the product between the remanence (B_r) and coercivity field. As seen from Fig. 5 and Fig. 6, the changing trend of $(BH)_{max}$ is agreement with that of the magnetic induction coercivity (H_{cb}).

Conclusions

In the work, the M-type Ca-Sr hexaferrites with composition of $Ca_{0.2}Sr_{0.8}Fe_{12.0-x}Ni_xO_{19}$ ($0.0 \leq x \leq 0.8$) were synthesized by the solid-state reactions. The microstructural and magnetic properties of the Ni substituted M-type Ca-Sr hexaferrites have been carefully investigated. The major findings of this work were listed in the following:

1. The results of X-ray diffraction patterns show that for the M-type hexaferrite magnetic powders with the Ni content (x) from 0.0 to 0.4, the XRD patterns belong to the M-type strontium hexaferrite; when Ni content (x) $\geq$ 0.6, $Sr_4Fe_6O_{13}$ is detected. It is observed that lattice parameter c first increases with the increase of Ni content (x) from 0 to 0.4, and then decreases when Ni content (x) $\geq$ 0.4, while lattice parameter a basically keeps constant. The c/a ratios of M-type hexaferrites first slightly increases with increasing Ni content (x) from 0.0 to 0.4, and then decreases when Ni content (x) $\geq$ 0.4.

2. Magnetization properties were measured at room temperature by a permanent magnetic measuring system. B_r first increases with increasing Ni content (x) from 0.0 to 0.2, and then decreases when Ni content (x) $\geq$ 0.2. H_{cj}, H_{cb} and $(BH)_{max}$ decrease with the increase of Ni content (x) from 0 to 0.8.

Acknowledgments

This work was supported by National Natural Science Foundation of China (No. 51272003 and No. 51472004), Scientific Research Fund of SiChuan Provincial Education Department (No. 13ZA0918, No. 14ZA0267 and No. 16ZA0330), the Major Project of Yibin City of China (No. 2012SF034 and No. 2016GY025), Scientific Research Key Project of Yibin

University (No. 2015QD13) and the Open Research Fund of Computational Physics Key Laboratory of Sichuan Province, Yibin University (No. JSWL2015KFZ04).

References

1. R.C. Pullar, Prog. Mater. Sci. 57 (2012) 1191-1334.
2. D. Seifert, J. Töpfer, F. Langenhorst, J.-M Le Breton, H. Chiron, L. Lechevallier, J. Magn. Magn. Mater. 321 (2009) 4045-4051.
3. J.F. Wang, C.B. Ponton, I.R. Harris, J. Alloys Compd. 403 (2005) 104-109.
4. B.H. Bhat, B. Want, Appl. Phys. A 122 (2016) 148.
5. R. Ezhil Vizhi, V. Harikrishnan, P. Saravanan, D. Rajan Bahu, J. Cryst. Growth 452 (2016) 117-124.
6. P. Sharma, R.A. Rocha, S.N. de Medeiros, B. Hallouche, A. Paesano Jr, J. Magn. Magn. Mater. 316 (2007) 29-33.
7. Y.J. Yang, F.H. Wang, X.S. Liu, J.X. Shao, D.H. Huang, J. Magn. Magn. Mater. 421 (2017) 349-354.
8. Y.J. Yang, X.S. Liu, D.L. Jin, Y.Q. Ma, Mater. Res. Bull. 59 (2014) 37-41.
9. Y.J. Yang, X.S. Liu, Mater. Technol. 29 (2014) 232-236.
10. Z.F. Zi, Q.C. Liu, J.M. Dai, Y.P. Sun, Solid State Commun. 152 (2012) 894-897.
11. R. Joshi, C. Singh, D. Kaur, H. Zaki, S.B. Narang, R. Jotania, S. Mishra, J. Singh, P. Dhruv, M. Ghimiree, J. Alloys Compd. 695 (2017) 909-914.
12. S. Shakoor, M.N. Ashiq, M.A. Malana, A. Mahmood, M.F. Warsi, M. Najam-ul-Haq, N. Karamat, J. Magn. Magn. Mater. 362 (2014) 110-114.
13. Y.M. Kang, Y.H. Kwon, M.H. Kim, D.Y. Lee, J. Magn. Magn. Mater. 382 (2015) 10-14.
14. M.N. Ashiq, M.J. Iqbal, I.H. Gul, J. Magn. Magn. Mater. 323 (2011) 259-263.
15. M.N. Ashiq, S. Shakoor, M. Najam-ul-Haq, M.F. Warsi, I. Ali, I. Shakir, J. Magn. Magn. Mater. 374 (2015) 173-178.
16. R.S. Alam, M. Moradi, M. Rostami, H. Nikmanesh, R. Moayedi, Y. Bai, J. Magn. Magn. Mater. 381 (2015) 1-9.
17. M.V. Rane, D. Bahadur, A.K. Nigam, C.M. Srivastava, J. Magn. Magn. Mater. 192 (1999) 288-296.
18. Y.J. Yang, J.X. Shao, F.H. Wang, X.S. Liu, D.H. Huang, Appl. Phys. A 123 (2017) 309.